# HYBRID MATERIALS BASED ON MODIFIED PECTIN AND HALLOYSITE FOR 3D PRINTING

Mădălina-Cristina NICOLAE[1], Sorina-Alexandra GÂREA[2], George-Mihail VLĂSCEANU[3], Cristina-Elena STAVARACHE[4], Celina-Maria DAMIAN[5], Horia IOVU[6]

*The aim of the present study is to develop a new bioink based on modified pectin and halloysite. For this purpose, different compositions of modified pectin with various halloysite concentrations (1 and 3 wt.%) were tested. NMR results confirmed modification of pectin. Rheological study highlighted the influence of halloysite on the polymeric matrix, while XPS results proved the hybrid nature of inks. The porosity of the scaffolds was evaluated through micro-CT and swelling investigation demonstrated the influence of scaffold porosity.*

**Keywords**: biomaterial ink, 3D printing, pectin, halloysite, porosity

## 1. Introduction

3D printing represents the method of manufacturing that enables obtaining complex objects with different sizes, shapes, and architecture in a layer-by-layer manner. This method was introduce in 2009, when Organovo marketed the first bioprinter (NovoGen MMX), a landmark moment for research involving the use of 3D printing in medical applications[1]. This increased interest was justified by the

[1] PhD student, Advanced Polymer Materials Group, Research Center for Advanced Materials, Products and Processes, National University of Science and Technology POLITEHNICA Bucharest, e-mail: madalina.nicolae@upb.ro

[2] Prof., Department of Bioresources and Polymer Science, Faculty of Chemical Engineering and Biotechnologies, Advanced Polymer Materials Group, National University of Science and Technology POLITEHNICA Bucharest, e-mail: sorina.garea@upb.ro

[3] Department of Bioengineering and Biotechnology, Faculty of Medical Engineering, Advanced Polymer Materials Group, National University of Science and Technology POLITEHNICA Bucharest, e-mail: vlasceanu.georgemihail@yahoo.ro

[4] Advanced Polymer Materials Group, Research Center for Advanced Materials, Products and Processes, National University of Science and Technology POLITEHNICA Bucharest, e-mail: cristina.stavarache@upb.ro

[5] Prof., Department of Bioresources and Polymer Science, Faculty of Chemical Engineering and Biotechnologies, Advanced Polymer Materials Group, National University of Science and Technology POLITEHNICA Bucharest, e-mail: celina.damian@yahoo.com

[6] Prof., Department of Bioresources and Polymer Science, Faculty of Chemical Engineering and Biotechnologies, Advanced Polymer Materials Group, National University of Science and Technology POLITEHNICA Bucharest, e-mail: horia.iovu@upb.com

need to develop personalized implants and devices adaptable to the anatomy of each patient. More recently, 3D bioprinting was proposed to be used for pharmaceutical printing for different routes of administration[2]. In 2015, Food and Drug Administration (FDA) approved the first pharmaceutical product, Spritam, an antiepileptic drug obtained by 3D printing. This processing technique offers the advantage of adapting the active ingredient dosage and drug release profile by choosing a specific designed and filling grade of the object in order to minimize side effects[3].

Microextrusion and fused deposition modeling (FDM) are the most used extrusion-based 3D printing techniques due to their simplicity and versatility. FDM requires the use of a synthetic polymer filament, which is melted in order to be deposited on the platform[4]. The high temperature required to melt the filament can cause damage to the active ingredient. In this regard, microextrusion is more friendly because it can use solutions of natural polymers that are placed in a syringe and, by using a pneumatic or mechanical force, are extruded through the nozzle. Extrusion-based printing with natural polymers was proposed for manufacturing of oral drug formulations of various active substances such as methylene blue in a mixture of cellulose and pectin[5], curcumin in alginate-celullose nanofibers[6] and, theophylline anydrous in carboxymethyl cellulose[7].

The main cell walls of many plants, including apples and citrus, contain pectin, an anioinic polymer that includes α-1,4-linked galacturonic acid backbones with various side chain residues, such as homogalacturonan, rhamnogalacturonan I, and rhamnogalacturonan II. Pectin is available in two varieties based on the level of methylation[8].

The degree of methylation has a significant impact on pectin's solubility and gelation ability. In general, low methylation pectin (LMP) is soluble in water and can create ionotropic gels when divalent ions are present The physical interactions between metallic ions and carboxilic groups involve the formation of an "egg box" structure [8]. In the case of high methylation pectin (HMP) an acidic medium is required to promote dissolution (below the pectin's pKa, which is between 3.5 and 4.5) and induces gel when sugar molecules are present or by cold gelation mechanisms [9].

Pectin exhibits the advantage of being resistant at acidic pH and presents a specific form of degradation by enzymes that exist in specific flora of the colon, which recommend this polymer as a possible canditate for oral drug delivery [10]. Another advantage of pectin relates to its mucoadhesiveness and anti-inflammatory properties[11]. It was also demonstrated that pectin may present other benefits for health, like hypoglycemic, hypocholesterolemic, and anti-cancer effects [12]. Shear-thinning behavior, or a decrease in viscosity as the shear rate increases, is an advantage of pectin for 3D printing applications [13]. In their investigation on the

impact of pectin concentration on ink printability, Passamai et al. found that a 20% concentration offered the optimum shape maintenance [14].

Nanoclays are a class of aluminosilicate nanomaterials that are composed of silicon tetrahedral and aluminum octahedral units. Since ancient times, nanoclays have been employed in medicine because of their broad use, low cost, and hemostatic and wound-healing capabilities[15]. Additionally, because of their high specific surface area and ability for cation exchange, nanoclays have been widely used in medical applications such as medication administration and antidiarrhea[16].

It is well known that the mechanical and thermal characteristics of polymers are improved when the nanoclays are included within the polymer matrix to create nanocomposites [17]. Because of their thixotropic and shear-thinning properties, which enhance printability and shape fidelity, nanoclays are recommended as additives in 3D printing applications[18]. Halloysite is a tubular clay with water molecules between layers and a similar chemical composition $Al_2Si_2O_5(OH)_4 \cdot nH_2O$ (n = 2 or 4) with kaolin [19]. In the dried form, the space between walls is about 0.72 nm, with an external diameter of 50–80 nm, 10–15 nm in the internal diameters, and between 400 and 1000 nm in the lengths [20]. The external surface is negatively charged because of the siloxane groups in the outer space, whereas the inside surface is positively charged because of the aluminol groups[21]. Its tubular structure and versatility of its surface make halloysite a good candidate for a large variety of drug delivery systems. Halloysite nanotubes were used in different inks, including polylactic acid [22][23], alginate [21] [22] and chitosan[23] [24] due to his role to sustained release and to improve their rheological properties, making the shear-thinning to be more pronunced which facilitate the extrusion and promoting a gel-like system.

To our knowledge, the blends based on pectin and halloysite was never exploited as ink for 3D bioprinting applications. In the literature, various hybrid materials based on HNT and alginate [24][25][28][29], chitosan[26][27][30], gelatin and tragacanth gum blends [31]have been developed for 3D printing

In the present study, a new bioink formula based on HNT and pectin was proposed. The citrus pectin was modified with methacrylate groups in order to have a more stable 3D structure scaffolds with an additional crosslinking effect. The present study focused on the development of new hybrid inks for extrusion-based bioprinting based on metacrylated pectin (PecMA) and halloysite nanotubes. Different grades of infill were proposed in order to control the porosity.

## 2. Materials and methods

### 2.1 Materials

Citric pectin (Pec) was supplied from Alfa Aesar and used as received. Halloysite, glycidyl methacrylate, 2-Hydroxy-4′-(2-hydroxyethoxy)-2-methylpropiophenone (Irgacure 2959), absolute ethanol and hydrochloric acid were purchased from Sigma Aldrich.

### 2.2 Modification of pectin

Pec was methacrylated with glycidyl methacrylate using the protocol described by Adriano Reis [32]. Briefly, in the first step, pectin was dissolved in deionized water in order to prepare a polymer solution of 2.5% concentration and then the temperature was raised up to 60 ºC followed by adjustment of pH at 3.5 using a solution of 0.1 N HCl. In the next step, methacrylation process was performed for 24 h by adding 2.6 mL of glycidyl methacrylate, corresponding to a pectin: glycidyl methacrylate molar ratio of 1:0.11. The modified pectin was purified by precipitation with ethanol and then was dialyzed in deionized water for 5 days. For further storage and use, PecMA was lyophilized for 72 hours at -76 °C .

### 2.3 $^1$H-NMR evaluation

The NMR analysis was performed by dissolving 30 mg of sample (citric pectin and PecMA) in 1 mL $D_2O$. The $^1$H-NMR spectra were registered on a Bruker NMR 600 MHz Advance spectrometer. The NMR analysis was used for determine the degree of methacrylation of PecMA using the formula 1[33].

$$\boldsymbol{DM} = \frac{\frac{I_{H_a}+I_{H_b}}{2}+I_{H_c}}{I_{H_3}+I_{H_4}}\,(\%) \qquad (1)$$

where: $H_a$ and $H_b$ represent methylene groups of methacrylate functions, Hc represent methyl group of methacrylate function, $H_3$ and $H_4$ represents anomeric protons from third and fourth position in Pec backbone.

### 2.4 Inks development

Three types of inks were prepared by mixing PecMA 20% with HNT in different weight mass ratios (1:0, 1:1, and 1:3). HNT was dispersed in distilled water by using an ultrasonic sonotrode device. Then, PecMA was gradually added and stirred at 60 ºC for 4 hours. A stock solution of Irgacure 2959 of 50 mg/mL concentration was prepared in absolute ethanol. The required volume was added to the solution to have a concentration of 1% related to the polymer concentration.

The inks were abbreviated as follows: PecMA for ink consists of 20% PecMA, PHNT1 for the ink with 1 wt. % HNT, and PHNT3 for the ink with 3 wt.% HNT.

### 2.5 Rheology

At room temperature, rheological tests were conducted with a Kinexus Pro rheometer in plate-plate geometry (20 mm) with a 0.5 mm gap. Viscosity measurements were made between 0.01 and 100 $s^{-1}$ which is the shear rate interval. The thixotropic test was performed using three intervals, first at a shear rate of 0.1 $s^{-1}$ for 180 s which was attributed to rest viscosity, and then for 10 s at a shear rate of 100 $s^{-1}$ which was attributed to the shear rate in the needle tip during printing. The recovery rate was then calculated using the initial shear rate (0,1 $s^{-1}$). Amplitude sweeps were carried out in the 0.01 Pa–1000 Pa shear stress interval at a steady frequency of 1 Hz. The frequency sweep was carried out at a shear rate within the linear-viscoelastic region (LVR) between 0.01 Hz and 10 Hz. A water-lock system was used to keep hydrated samples during the measurements, which were conducted at room temperature (25 °C).

### 2.6 Design of 3D structure and printing process

Different types of 3D printed structures were designed using BioCAD software. Cylinders with a diameter of 12 mm, different heights (2.88 mm, 1.92 mm, and 1.44 mm) and different offsets (3, 2, and 1.5) were designed. The samples were denoted by adding the final numbers of resulting lines in the printed structure (3L for the height of 2.88 mm, 5L for 1.92 mm, and 7L for 1.44 height) at the name of the ink. The printing process was performed at room temperature on glass slides using a conical needle G25 with a speed of 4 mm/second with printing speed varied in the range of 285-300 kPa. The obtained 3D structures were exposed to a UV lamp (365 nm) for 30 minutes for the photocrosslinking process.

### 2.7 X-ray photoelectron spectroscopy (XPS)

X-ray photoelectron spectroscopy (XPS) analysis was conducted on a K-Alpha spectrometer with a monochromatic Al Kα source (1486.6eV) using a vacuum base pressure of $2 \times 10^{-9}$mbar.

### 2.8 micro-CT

In order to obtain micro-computer tomography images, a SkyScan μCT 1272 equipment was used. The freeze-dried samples were scan for 180º using a rotation step of 0.2º with a resolution of 5 μm. Scanning was performed without filter at 40 kV, 135 μA with a exposure time of 350 ms. NRecon software were used to build tomograms and CTAn software were used for quantitative measurements.

### 2.9 Swelling degree

The swelling degree was investigated in two different aqueous media: simulated gastric fluid (SGF) pH 1.2 and simulated intestinal fluid (SIF) pH 6.8. The dried 3D structures were weighed and then placed in SGF for two hours at 37 ºC, followed by changing with SIF. At predetermined times, the samples were removed and easily wiped off with filter paper and then the wet sample was weighed The swelling degree was calculated using Formula 2[34].

$$swelling\ degree\ (\%) = \frac{wet\ sample - dry\ sample}{dry\ sample} \times 100 \quad (2)$$

## 3. Results and discussion

### 3.1 $^1$H-NMR evaluation

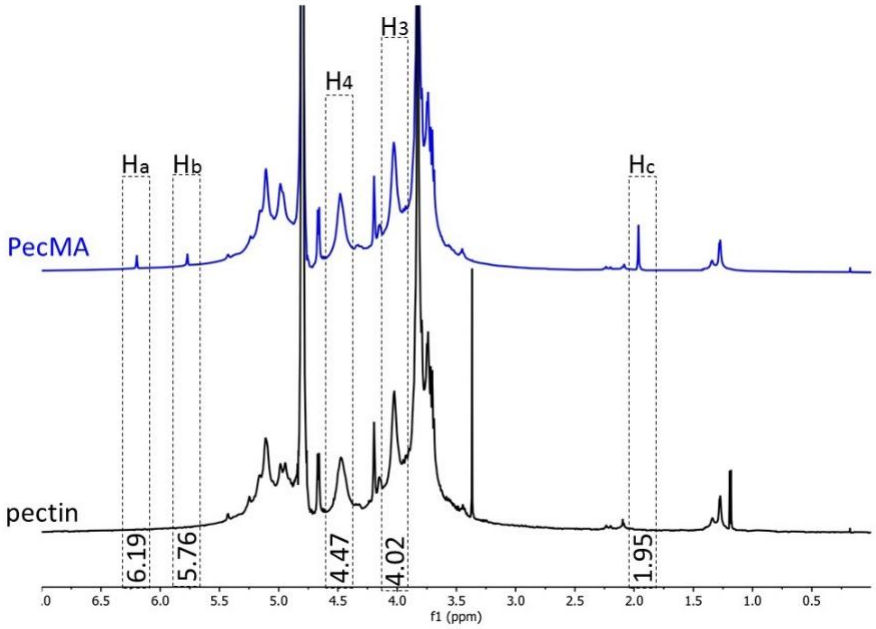


Fig. 1 - $^1$H-NMR spectra of citrius pectin and PecMA

$^1$H-NMR analysis was performed to investigate the modification of citric pectin with methacrylic groups. Fig. 1 shows the $^1$H-NMR spectrum of modified pectin in which new signals at 6.19 and 5.76 ppm corresponding to vinyl protons and a signal at 1.95 ppm, assigned to methyl, protons were detected [35]. The grade of methacrylation was estimated to be 5.77%.

A higher degree of methacrylation can affect the biocompatibility of the modified polymer matrix. Therefore, a lower degree of methacrylation can provide the suitable properties, such as structural stability and adequate mechanical performance, while preserving biocompatibility[36]. Moreover, an increased degree of methacrylation could also affect the hydrophilicity of the polymer, an important parameter for materials used in the biomedical applications[37][38].

### 3.2 Rheology

The most important rheological property of an ink suitable for extrusion through a needle is its shear-thinning behavior. Fig. 2 a) shows the viscosity plotted against the shear rate for the investigated inks. The rheological results indicate that all compositions exhibit a pronunced shear-thinning behavior, while the presence of HNT significantly influences the viscosity of the inks. The PecMA based ink presents the lowest viscosity, followed by PHNT3, while the PHNT1exhibits the highest viscosity across the entire shear rate range.

While shear-thinning governs ink flow during extrusion, thixotropic recovery is critical for the rebuilding of the internal structure after deposition. Thixotropy is a time-dependent shear-thinning behavior in which the ink behaves as a solid-like material at low shear rate and undergoes a transition to a liquid-like state under high shear rates[39]. Once the high shear rate is removed, rapid recovery of the initial internal structure is required to support the printed filament and maintain shape fidelity. In Fig. 2 b) can be observed the three-interval thixotropic tests revealed that after 10 seconds the PecMA, PHNT1, and PHNT3 ink have a recovery of 51.59%, 48.70%, and 53.98% respectively. After 1 minute the recovery was increasing to 77.83%, 67.99%, and 79.1%. It is considered that a recovery rate bigger than 60% is enough to support their height[6]. Among the investigated inks, PHNT3 exhibited the most balanced recovery behavior, suggesting an optimal compromise between flowability under shear and structural rebuiling at rest. Despite the fact that PHNT1 presents the highest viscosity, the recovery is slower due to a more rigid HNT-pectin network.

Amplitude, sweep test were performed to determine the linear-viscoelastic region (LVR), defined as the stress range in which the material structure remains intact. In Fig. 2 c) can be observed that all the inks present a gel-like behavior as evidenced by elastic modulus G' values consistently exceeding the loss modulus G" in all investigated interval. The addition of nanoclay favors an increase of both storage and loss modulus which indicates the reinforcement of polymeric matrix[40]. This enhancement can be attributed to the formation of hydrogen bonding and electrostatic interactions between $COO^-$ groups of pectin and oppositely charge edge and inner lumen of HNT. Similar behavior was reported in the case of alginate/HNT inks by Glukhova et al. [24], [25].

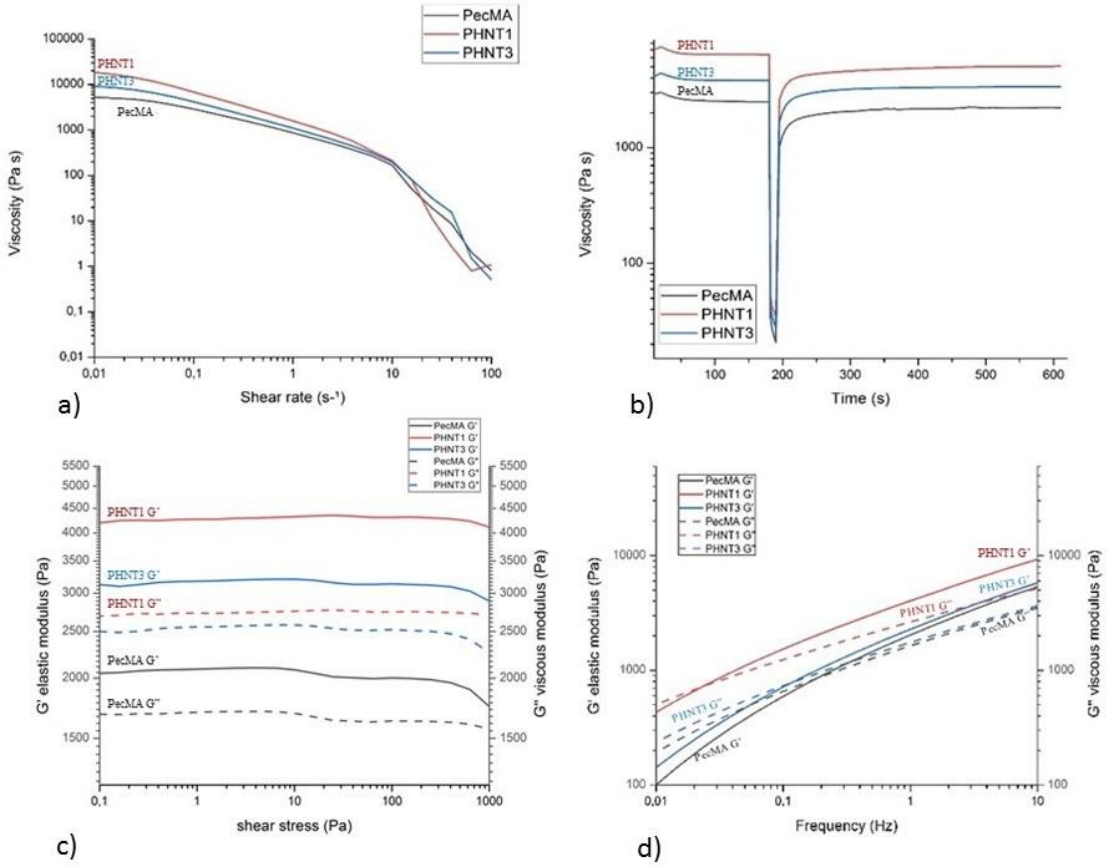


Fig. 2-Rheological investigations of inks based on PecMA and HNT

Regarding the frequency test (Fig. 2 d), the values of G' and G", for all inks, increased with the frequency. At very low-frequency, the loss modulus records higher values than storage modulus indicating a more liquid-like response under long-timescale[41]. As the frequnecy increased, G' became greater than G", demonstrating the transition toward a predominantly gel-like behavior. The value of loss tangent (Tan (δ)) were lower than 1, indicated a predominantly elastic response which is a crucial behavior that makes the inks retain the shape after deposition[42].

### 3.3 X-ray photoelectron spectroscopy (XPS)

Fig. 3 reveals the elemental composition of the samples surface. The XPS spectra recorded for the raw materials involved in the composition of the composite scaffolds confirm their different nature. In the case of HNT, the XPS spectrum is in agreement with the general formula of clay ($Al_2Si_2O_5(OH)_4 \cdot 4H_2O$.) indicating elements such as O (57.25 %), Si (18.01 %), Al (16.4 %) and some impurities (C

and Na) in a low concentration. As it was expected, the XPS analysis of modified pectin suggested a composition of specific organic nature by the presence of elements such as O (39.88 %) and C (59.17 %). A low amount of Na (0.95 %) was detected as an impurity.The survey data confirmed the hybrid nature of the inks (PHNT1 and PHNT3) by the appearance of the signal assigned for Si 2p.

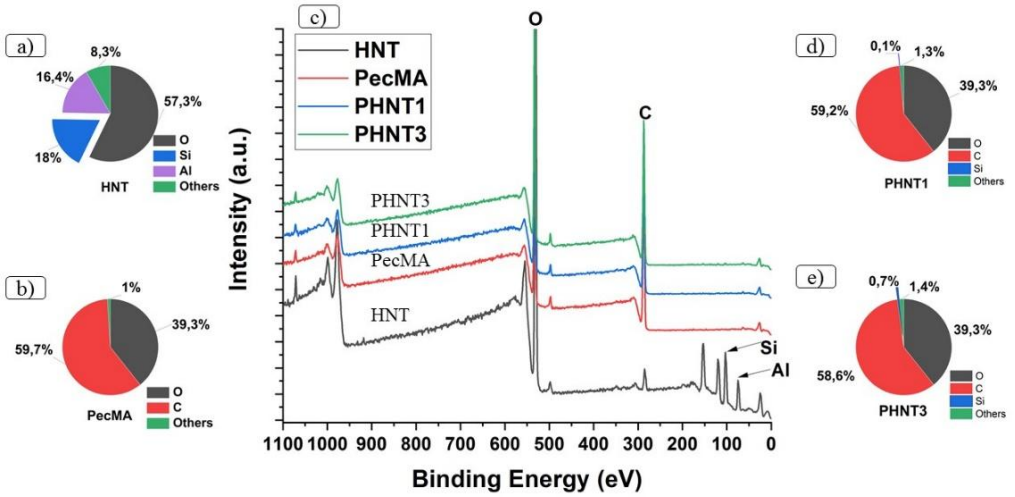


Fig. 3 – Survey XPS spectra of PecMA – HNT composite scaffolds

### 3.4 micro-CT

Fig. 4 shows representative morphologies of the 3D printed structures obtained from micro-CT analysis. As shown, the addition of HNT strongly influences the internal architecture of the printed scaffolds. The PecMA sample presents smooth walls (Fig. 4 a), whereas the addition of HNT leads to the appearance of roughness walls which are particularly pronunced in the PHNT3 sample (Fig. 4 c). The PHNT1 printed structure exhibits circular and irregular pores, resulting from partial filament collapse after printing. In contrast, the printed structures based on PecMA and PHNT3 largely preserve the intended square lattice architecture.

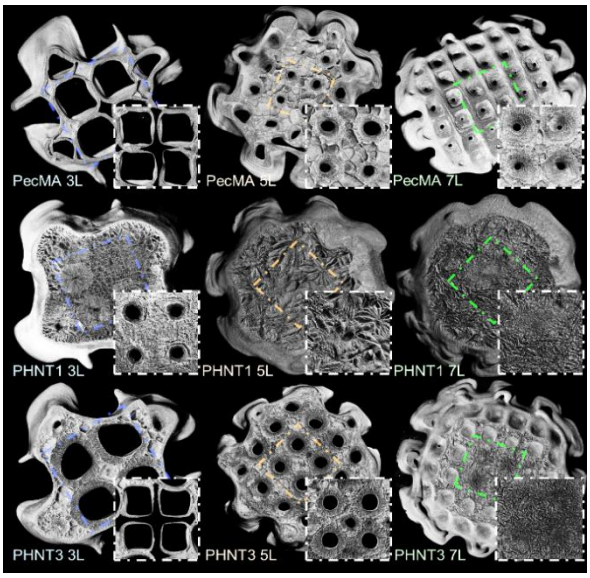


Fig. 4-Cross-sectional analysis of 3D printed structures. Main images (uppercase CS 1-9) display the porous internal structure, while the corner subsets (lowercase cs 1- 9) focus on the central grid areas at a different depth.

The total porosity of each printed samples is depicted in Fig. 5 a) and, calculated as the ratio between the total pore volume and the overall volume of the printed structure, including square lattice architecture. As can be observed in the case of PecMA and PHNT3, the total porosity varies according to the projected CAD model. In contrast, for the PHNT1 sample, the total porosity did not decrease as expected, which can be attributed to fillament collapse occurring after printing. In the Figs. 5 b), d), f) are shown the distribution of wall thickness, while in c), e), g) are presented the distribution of pore size. In the PecMA sample, both wall thickness and pores size exhibit a highly uniform distribution across the entire dimensional range. The high percentage of pores with dimensions in the range of 505-1005 µm, in the case of PecMA 3L, was attributed to the created pores in the CAD model. The PHNT1 sample exhibits a very narrow pore size distribution, with a high percent in the range of 5-55 µm. The low fraction of large pores is consistent with previously discussed filament collapse occurring after depositions. In contrast, the PHNT3 samples are characterized by a more uniform over the entire dimensional range, similar to that observed for PecMA samples. Compared to PecMA 3L, where the dominant pore size range is 505-1005 µm, PHNT3 exhibits larger pores predominantly in the 1005-1505 µm range, indicating an improved preservation of the designed CAD architecture. This result is in good agreement with the rheological data, particularly the thixotropic recovery behavior.

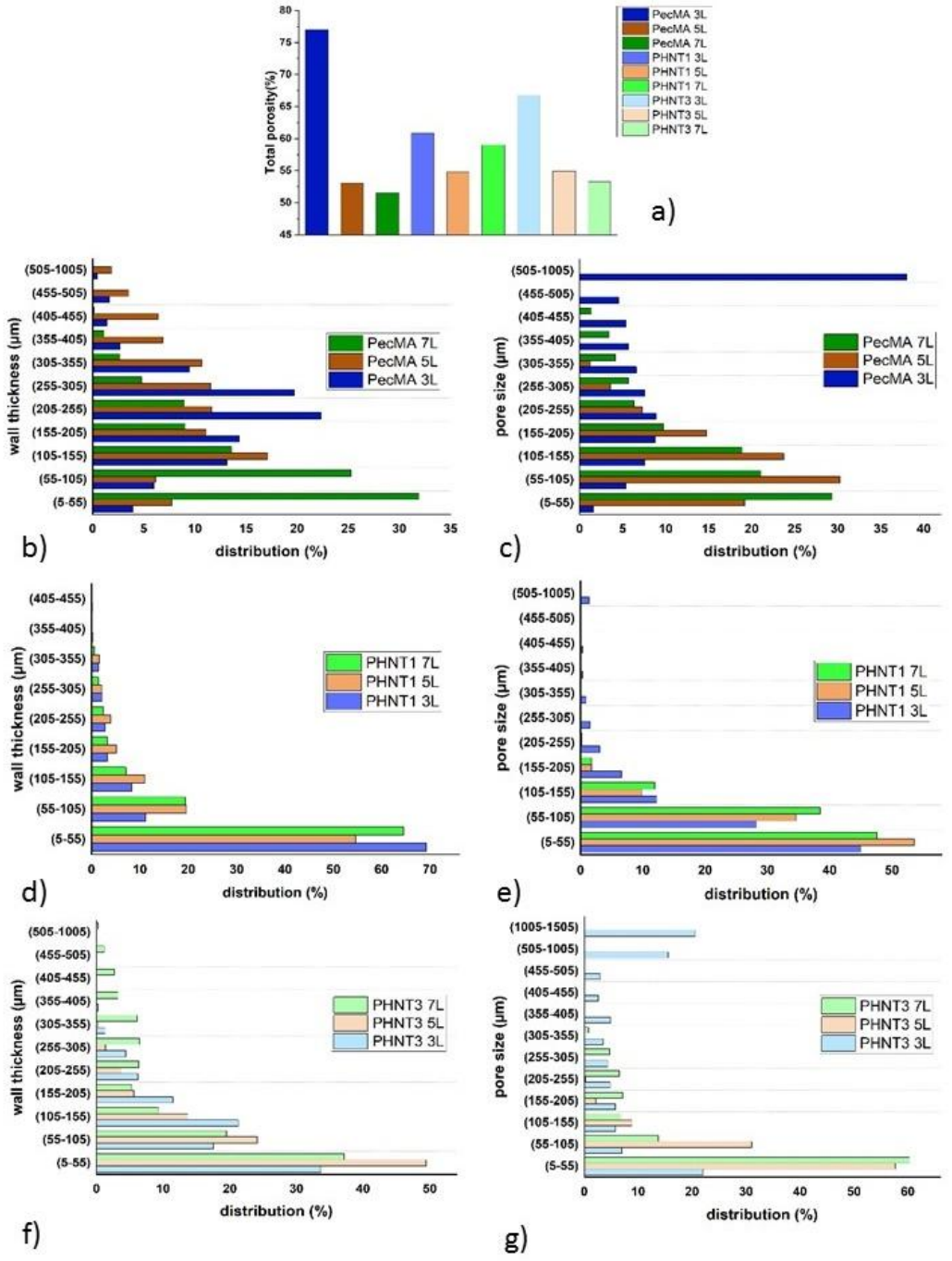


Fig. 5 – Morphometrical analysis of the 9 3D printed objects. a) total porosity; b) ) wall thickness distribution in PecMA batch, d) wall thickness distribution in PHNT1 batch, f) wall thickness distribution in PHNT3 batch; c) pore diameter distribution in PecMA batch, e) pore diameter distribution in PHNT1 batch, g) pore diameter distribution in PHNT3 batch

### 3.5 Swelling degree

The swelling behavior of the printed scaffols was investigated in different media (Fig. 6).

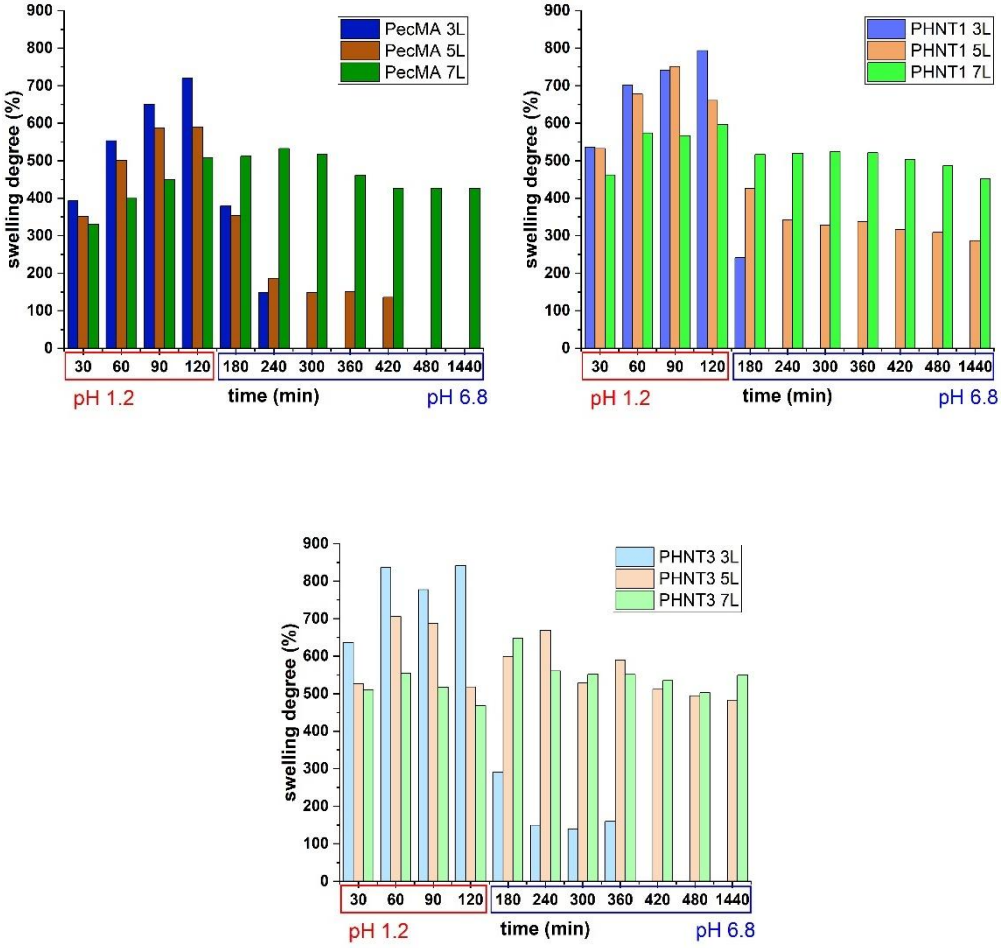


Fig. 6-Swelling degree of PecMA-HNT hydrogels in pH 1.2 and 6.8 at different periods of time

Initially, the 3D structures were immersed in a simulated gastric fluid (SGF) characterized by an acidic pH value (1.2) for 2 hours and then the medium was changed with simulated intestinal fluid (SIF) with a pH value of 6.8 to mimic the exposure through the gastro-intestinal tract. The results indicated that the swelling degree increased with the addition of HNT. One possible explanation can be attributed to the high water-absorption capacity of nanoclay [43]. Also can be observed that the porosity influences the swelling degree, the samples with the

highest porosity (PecMA 3L, PHNT1 3L, PHNT3 3L) present the highest swelling degree. After 240 minutes of immersion in an aqueous medium, the samples with high and medium distances between strands began to mechanically disintegrate which demonstrates that the porosity also influences the degradation process. The fast degradation of porous sample can be attributed to the large surface exposed to the medium which was also observed by Tabriz et al[44]. After 30 minutes of immersion in SGF, the samples with small offset (small porosity) – PecMA 7L, PHNT1 7L, and PHNT3 7L present a swelling degree of 330%, 461%, and 509%, respectively. After 1440 minutes the previously mentioned samples presented a swelling degree of 426%, 451%, and 549%. In the case of the PecMA and PHNT1 (PecMA 3L, PHNT1 3L, PecMA 5L, PHNT1 5L), the swelling process is faster in SIF compared to SGF probably due to the more porous structure of the scaffolds. The samples with similar compositions, but with a lower porosity (PecMA 7L, PHNT1 7L), present similar swelling behavior in SIF and SGF. The PHNT3 sample behave a little bit differently in SIF and SGF in comparison with PecMA and PHNT1. The low porous PHNT3 7L present a more swelling in SIF comparative with SGF. The PHNT3 5L presents similar swelling in SIF and SGF. The high porous PHNT3 3L present a very pronunced decrease in swelling after in SIF compared with SGF.

## 4. Conclusions

In this study, we proposed new hybrid inks based on methacrylated pectin (PecMA) and halloysite (HNT) for extrusion-based 3D printing. The experimental results indicated the influence of HNT on the structural stability, porosity and degradation of the printed structures by characterization of biomaterials from rheological, structural, and swelling perspectives. The porosity of the 3D printed structures was investigated in a non-destructive manner by micro-tomography and highlighted that low HNT concentrations (1 and 3 wt. %) within PecMA influences the porosity of composite scaffolds. In addition, the internal structure and printing fidelity are both enhanced by the addition of HNT to the PecMA matrix. The results of micro-CT analysis are in agreement with the rheological data regarding the flow behavior of the inks. The samples characterized by the highest porosity showed a very quick mechanical disintegration due to their large surface which is exposed. The swelling behavior of hybrid scaffolds, in simulated fluids (SGF and SIF), demonstrated the application potential of these 3D printed structures in drug delivery field in which the porosity represents a key factor that are involved in the drug release profile.

**Acknowledgments**:

This research study was supported by a National Research Grant - ARUT, contract no. 23/09.10.2023, *New smart hydrogels based on biopolymers and graphene oxide for photothermal therapy*.

## REFERENCES

[1] H. Cui, M. Nowicki, J. P. Fisher, and L. G. Zhang, "3D Bioprinting for Organ Regeneration.," Adv. Healthc. Mater., vol. 6, no. 1, Jan. 2017.

[2] A. Mihaylova, D. Shopova, N. Parahuleva, A. Yaneva, and D. Bakova, "(3D) Bioprinting—Next Dimension of the Pharmaceutical Sector," Pharmaceuticals, vol. 17, no. 6. 2024.

[3] N. Sultana, A. Ali, A. Waheed, and M. Aqil, "3D Printing in pharmaceutical manufacturing: Current status and future prospects," Mater. Today Commun., vol. 38, p. 107987, 2024.

[4] S. Cailleaux, N. M. Sanchez-Ballester, Y. A. Gueche, B. Bataille, and I. Soulairol, "Fused Deposition Modeling (FDM), the new asset for the production of tailored medicines," J. Control. Release, vol. 330, pp. 821–841, 2021.

[5] P. Panraksa et al., "Characterization of Hydrophilic Polymers as a Syringe Extrusion 3D Printing Material for Orodispersible Film," Polymers (Basel)., vol. 13, no. 20, 2021.

[6] R. Olmos-Juste, O. Guaresti, T. Calvo-Correas, N. Gabilondo, and A. Eceiza, "Design of drug-loaded 3D printing biomaterial inks and tailor-made pharmaceutical forms for controlled release," Int. J. Pharm., vol. 609, p. 121124, 20214.

[7] P. Panraksa et al., "Sustainable 3D printing of oral films with tunable characteristics using CMC-based inks from durian rind wastes," Eur. J. Pharm. Biopharm., vol. 186, pp. 30–42, 2023.

[8] P. Ishwarya S., S. R., and P. Nisha, "Advances and prospects in the food applications of pectin hydrogels," Crit. Rev. Food Sci. Nutr., vol. 62, no. 16, pp. 4393–4417, Jun. 2022.

[9] N. S. Bostancı, S. Büyüksungur, N. Hasirci, and A. Tezcaner, "Potential of pectin for biomedical applications: a comprehensive review," J. Biomater. Sci. Polym. Ed., vol. 33, no. 14, pp. 1866–1900, Sep. 2022.

[10] M. Khotimchenko, "Pectin polymers for colon-targeted antitumor drug delivery," Int. J. Biol. Macromol., vol. 158, pp. 1110–1124, 2020.

[11] F. Patitucci et al., "3D-Printed Alginate/Pectin-Based Patches Loaded with Olive Leaf Extracts for Wound Healing Applications: Development, Characterization and In Vitro Evaluation of Biological Properties," Pharmaceutics, vol. 16, no. 1, 2024.

[12] D. Li et al., "Pectin in biomedical and drug delivery applications: A review," Int. J. Biol. Macromol., vol. 185, pp. 49–65, 2021, doi: https://doi.org/10.1016/j.ijbiomac.2021.06.088.

[13] M. Pitton, A. Fiorati, S. Buscemi, L. Melone, S. Farè, and N. Contessi Negrini, "3D Bioprinting of Pectin-Cellulose Nanofibers Multicomponent Bioinks," Front. Bioeng. Biotechnol., vol. 9, 2021.

[14] V. E. Passamai, S. Katz, B. Rodenak-Kladniew, V. Alvarez, and G. R. Castro, "Pectin-based inks development for 3D bioprinting of scaffolds," J. Polym. Res., vol. 30, no. 1, p. 35, 2022.

[15] K. S. Katti, H. Jasuja, S. V Jaswandkar, S. Mohanty, and D. R. Katti, "Nanoclays in medicine: a new frontier of an ancient medical practice," Mater. Adv., vol. 3, no. 20, pp. 7484–7500, 2022.

[16] Y. Feng et al., "A ferroptosis-targeting ceria anchored halloysite as orally drug delivery system for radiation colitis therapy," Nat. Commun., vol. 14, no. 1, p. 5083, 2023.

[17] M. S. Saharudin, S. Hasbi, M. N. A. Nazri, and F. Inam, "A Review of Recent Developments

in Mechanical Properties of Polymer–Clay Nanocomposites," in Advances in Manufacturing Engineering, 2020, pp. 107–129.

[18] F. García-Villén et al., "Clay Minerals as Bioink Ingredients for 3D Printing and 3D Bioprinting: Application in Tissue Engineering and Regenerative Medicine," Pharmaceutics, vol. 13, no. 11, 2021.

[19] M. Fizir, P. Dramou, N. S. Dahiru, W. Ruya, T. Huang, and H. He, "Halloysite nanotubes in analytical sciences and in drug delivery: A review," Microchim. Acta, vol. 185, no. 8, p. 389, 2018.

[20] L. Peña-Parás, J. A. Sánchez-Fernández, and R. Vidaltamayo, "Nanoclays for Biomedical Applications BT - Handbook of Ecomaterials," L. M. T. Martínez, O. V. Kharissova, and B. I. Kharisov, Eds. Cham: Springer International Publishing, 2017, pp. 1–19.

[21] M. Massaro, R. Noto, and S. Riela, "Past, Present and Future Perspectives on Halloysite Clay Minerals.," Molecules, vol. 25, no. 20, Oct. 2020.

[22] J. A. Weisman, U. Jammalamadaka, K. Tappa, and D. K. Mills, "Doped Halloysite Nanotubes for Use in the 3D Printing of Medical Devices," Bioengineering, vol. 4, no. 4. p. 96, 2017.

[23] Y. Luo, A. Humayun, and D. K. Mills, "Surface Modification of 3D Printed PLA/Halloysite Composite Scaffolds with Antibacterial and Osteogenic Capabilities," Applied Sciences, vol. 10, no. 11. p. 3971, 2020.

[24] S. A. Glukhova, V. S. Molchanov, Y. M. Chesnokov, B. V Lokshin, E. P. Kharitonova, and O. E. Philippova, "Green nanocomposite gels based on binary network of sodium alginate and percolating halloysite clay nanotubes for 3D printing," Carbohydr. Polym., vol. 282, p. 119106, 2022.

[25] S. A. Glukhova et al., "Printable Alginate Hydrogels with Embedded Network of Halloysite Nanotubes: Effect of Polymer Cross-Linking on Rheological Properties and Microstructure," Polymers (Basel)., vol. 13, no. 23, 2021.

[26] Y. Liu et al., "Designing and utilizing 3D printed chitosan/halloysite nanotubes/tea polyphenol composites to maintain the quality of fresh blueberries," Innov. Food Sci. Emerg. Technol., vol. 74, p. 102808, 2021.

[27] Y. Wang et al., "Preparation, characterization, and 3D printing verification of chitosan/halloysite nanotubes/tea polyphenol nanocomposite films," Int. J. Biol. Macromol., vol. 166, pp. 32–44, 2021.

[28] Y. Zhou, X. Gao, M. Zhao, L. Li, and M. Liu, "Three-dimensional printed sodium alginate clay nanotube composite scaffold for bone regeneration," Compos. Sci. Technol., vol. 250, p. 110537, 2024.

[29] B. R. Zineh, L. Roshangar, S. Meshgi, and M. Shabgard, "3D printing of alginate/thymoquinone/halloysite nanotube bio-scaffolds for cartilage repairs: experimental and numerical study," Med. Biol. Eng. Comput., vol. 60, no. 11, pp. 3069–3080, 2022.

[30] X. Chen et al., "3D printing of chitosan hydrogel reinforced with tubular nanoclay for hemostasis and infected wound healing," Bioact. Mater., vol. 54, pp. 404–422, 2025.

[31] H. Zehtab Minooei and B. Kaffashi, "Viscoelastic properties of thermosensitive gelatin/tragacanth hydrogel as novel ink suitable for additive manufacturing: Effect of various additives on system's viscoelastic characteristics and printability," J. Appl. Polym. Sci., vol. 140, no. 34, p. e54328, Sep. 2023.

[32] A. V Reis, M. R. Guilherme, A. T. Paulino, E. C. Muniz, L. H. C. Mattoso, and E. B. Tambourgi, "Synthesis of Hollow-Structured Nano- and Microspheres from Pectin in a Nanodroplet Emulsion," Langmuir, vol. 25, no. 4, pp. 2473–2478, Feb. 2009.

[33] R. F. Pereira, A. Sousa, C. C. Barrias, P. J. Bártolo, and P. L. Granja, "A single-component hydrogel bioink for bioprinting of bioengineered 3D constructs for dermal tissue engineering," Mater. Horizons, vol. 5, no. 6, pp. 1100–1111, 2018.

[34] S. Gupta and A. Bit, "16 - Rapid prototyping for polymeric gels," in Woodhead Publishing Series in Biomaterials, K. Pal and I. B. T.-P. G. Banerjee, Eds. Woodhead Publishing, 2018, pp. 397–439.
[35] J. C. O. Villanova, E. Ayres, and R. L. Oréfice, "Design, characterization and preliminary in vitro evaluation of a mucoadhesive polymer based on modified pectin and acrylic monomers with potential use as a pharmaceutical excipient," Carbohydr. Polym., vol. 121, pp. 372–381, 2015.
[36] X. Jiao et al., "The Preparation and Potential Bioactivities of Modified Pectins: A Review," Foods, vol. 12, no. 5. p. 1016, 2023.
[37] A. S. Hoffman, "Hydrogels for biomedical applications," Adv. Drug Deliv. Rev., vol. 64, pp. 18–23, 2012.
[38] A. I. Van Den Bulcke, B. Bogdanov, N. De Rooze, E. H. Schacht, M. Cornelissen, and H. Berghmans, "Structural and Rheological Properties of Methacrylamide Modified Gelatin Hydrogels," Biomacromolecules, vol. 1, no. 1, pp. 31–38, Mar. 2000.
[39] C. C. Clark, J. Aleman, L. Mutkus, and A. Skardal, "A mechanically robust thixotropic collagen and hyaluronic acid bioink supplemented with gelatin nanoparticles," Bioprinting, vol. 16, p. e00058, 2019.
[40] A. Sheikhi, S. Afewerki, R. Oklu, A. K. Gaharwar, and A. Khademhosseini, "Effect of ionic strength on shear-thinning nanoclay-polymer composite hydrogels.," Biomater. Sci., vol. 6, no. 8, pp. 2073–2083, Jul. 2018.
[41] Á. D. Virág, Z. Juhász, A. Kossa, and K. Molnár, "Combining oscillatory shear rheometry and dynamic mechanical analysis to obtain wide-frequency master curves," Polymer (Guildf)., vol. 295, p. 126742, 2024.
[42] Y. Chen et al., "3D Bioprinting of shear-thinning hybrid bioinks with excellent bioactivity derived from gellan/alginate and thixotropic magnesium phosphate-based gels," J. Mater. Chem. B, vol. 8, no. 25, pp. 5500–5514, 2020.
[43] W. Wu et al., "Fabricating of poly(vinyl alcohol)/halloysite nanotubes/gelatin composite sponges with enhanced mechanical properties and rapid water absorption speed," Polym. Eng. Sci., vol. 64, no. 2, pp. 641–652, Feb. 2024.
[44] A. G. Tabriz et al., "Personalised paediatric chewable Ibuprofen tablets fabricated using 3D micro-extrusion printing technology," Int. J. Pharm., vol. 626, p. 122135, 2022.